



Published in final edited form as:

Biomaterials. 2006 February ; 27(5): 735–744. doi:10.1016/j.biomaterials.2005.06.020.

Microintegrating smooth muscle cells into a biodegradable, elastomeric fiber matrix

John J. Stankus^{a,c}, Jianjun Guan^c, Kazuro Fujimoto^c, and William R. Wagner^{a,b,c,*}

^aDepartment of Chemical Engineering, 100 Technology Drive, University of Pittsburgh, Pittsburgh, PA 15261, USA

^bDepartment of Bioengineering, 100 Technology Drive, University of Pittsburgh, Pittsburgh, PA 15261, USA

^cMcGowan Institute for Regenerative Medicine, 100 Technology Drive, University of Pittsburgh, Pittsburgh, PA 15219, USA

Abstract

Electrospinning permits fabrication of biodegradable elastomers into matrices that can resemble the scale and mechanical behavior of the native extracellular matrix. However, achieving high-cellular density and infiltration with this technique remains challenging and time consuming. We have overcome this limitation by electrospaying vascular smooth muscle cells (SMCs) concurrently with electrospinning a biodegradable, elastomeric poly(ester urethane)urea (PEUU). Trypan blue staining revealed no significant decrease in cell viability from the fabrication process and electrospayed SMCs spread and proliferated similar to control unprocessed SMCs. The resulting SMC microintegrated PEUU constructs were cultured under static conditions or transmural perfusion. Higher cell numbers resulted with perfusion culture with 131% and 98% more viable cells versus static culture at days 4 and 7 ($p < 0.05$). Fluorescent imaging and hematoxylin and eosin staining further illustrated high cell densities integrated between the elastomeric fibers after perfusion culture. SMC microintegrated PEUU was strong, flexible and anisotropic with tensile strengths ranging from 2.0 to 6.5 MPa and breaking strains from 850 to 1700% dependent on the material axis. The ability to microintegrate smooth muscle or other cell types into a biodegradable elastomer fiber matrix embodies a novel tissue engineering approach that could be applied to fabricate high cell density elastic tissue mimetics, blood vessels or other cardiovascular tissues.

Keywords

Bioreactor; Smooth muscle cell; Elastomer; Electrospinning; Polyurethane; Scaffold

1. Introduction

Highly cellularized and mechanically functional engineered tissue constructs are desired to repair or replace diseased cardiovascular and other soft tissues. A typical method to create such constructs involves fabricating biodegradable porous scaffolds that are subsequently seeded with cells, cultured in vitro, and then implanted. While synthetic or processed natural material scaffolds can provide some mechanical support, the use of load bearing scaffolds often is coupled with long cell seeding and culture times to achieve high cellular densities in

*Corresponding author. Tel.: +412 235 5138; fax: +412 235 5110. wagnerwr@upmc.edu (W.R. Wagner).

the scaffold and adequate mechanical properties for in vivo transplantation [1,2]. Mechanically robust, contractile muscle or cardiovascular tissues consist of high densities of aligned cell morphologies. To fabricate functional tissue, it is also desired that scaffolds are designed to both support cell–cell interactions as well as to direct cell alignment in mimicking this tissue structure.

The method of electrospinning, originally patented in the 1930s, has recently experienced renewed interest for tissue engineering applications [3–5]. Electrospinning is attractive to the tissue engineering community in that it permits fabrication of scaffolds that resemble the scale and fibrous nature of the native extracellular matrix (ECM). The ECM is composed of fibers, pores, and other surface features at the sub-micron and nanometer size scale. Many believe that such nanoscale features directly impact cellular interactions with synthetic materials such as migration and orientation [6,7]. Electrospinning also permits fabrication of oriented fibers to result in scaffolds with inherent anisotropy. These aligned scaffolds can influence cellular growth, morphology and ECM production. For example, Xu et al. found smooth muscle cell (SMC) alignment with poly(L-lactide-co-ε-caprolactone) fibers [8] and Lee et al. submitted aligned non-biodegradable polyurethane to mechanical stimulation and found cells cultured on aligned scaffolds produced more ECM than those on randomly organized scaffolds [9].

While electrospinning can fabricate scaffolds that possess an ECM-like fibrous structure, this morphology also results in pore sizes that are generally smaller (< 50 μm) and more tortuous than those produced by other scaffold methods such as salt leaching and thermally induced phase separation [10]. Therefore, methods to seed high densities of cells into scaffolds such as vacuum filtration [11] are not effective in achieving a uniform distribution throughout a thick construct. It has been suggested that cells statically seeded on electrospun matrices can migrate into the interior by displacing or enzymatically degrading individual fibers in the process [4]. While this may be possible, an extended culture period and appropriate signals for cell migration into thick construct interiors might also be required. To overcome this problem and achieve a highly cellularized tissue engineered construct while also providing elastomeric mechanical support, we have developed a microintegration approach wherein a meshwork of sub-micron elastomeric fibers is electrospun concurrent with cellular placement. The constructs fabricated by this method were characterized for fiber and cell morphologies, mechanical properties, and cell viability and proliferation.

After seeding scaffolds with high cell densities it is important to provide sufficient nutrient and waste transfer to preserve cell viability and support proliferation. Reports have shown that nutrient transport is often limited to diffusion alone [12]. Diffusion usually proves sufficient for relatively thin scaffolds of 100–200 μm. However, with thicker scaffolds (> 200 μm) tissue development can be limited. Transmural perfusion has been shown to result in increased cell density and uniformity within cultured scaffolds [13]. Therefore, we have employed a perfusion bioreactor similar in design to that reported by Radisic et al. [13] to provide significant media convection for high density SMC growth in our microintegrated constructs.

The objective of this study was to investigate the process of SMC microintegration into electrospun poly(ester urethane)urea (PEUU). A previously developed biodegradable and cytocompatible PEUU based on polycaprolactone diol, 1,4-diisocyanatobutane, and putrescine was utilized as the elastomeric fiber material [14]. Cellular viability as a function of the cellular incorporation method was studied using Trypan blue staining. An electrospinning apparatus previously described [15] was modified to produce mechanically robust SMC microintegrated scaffolds that were cultured statically or in a trans-mural perfusion bioreactor. Cell growth and morphology within the elastomeric fiber matrices

were evaluated. Tensile mechanical properties were measured following the microintegration process.

2. Materials and methods

2.1. Polymer synthesis and characterization

1,4-diisocyanatobutane (BDI, Fluka) and putrescine (Sigma) were distilled under vacuum. Polycaprolactone diol (PCL, $MW = 2000$, Aldrich) was vacuum dried for 48 h. Dimethyl sulfoxide (DMSO) and *N,N*-dimethylformamide (DMF) were dried over 4-Å molecular sieves. Stannous octoate (Sigma) and hexafluoroisopropanol (HFIP, Oakwood Products) were used as obtained.

Cytocompatible and biodegradable PEUU was synthesized from PCL and BDI with subsequent chain extension by putrescine as reported previously [14]. The reaction consisted of a two-step solution polymerization in DMSO using a 2:1:1 BDI: PCL: putrescine mole ratio. PEUU cast films were prepared from a 3 wt% solution in DMF and dried under vacuum for 48 h. PEUU was characterized for molecular weight, thermal transitions and uniaxial tensile properties as described previously [15].

2.2. Electrospinning

PEUU was electrospun using a technique similar to that previously described [15]. In brief, PEUU was dissolved in HFIP under mechanical stirring at either 5 or 12 wt%. The PEUU solution was fed at 1.5 mL/h using a syringe pump (Harvard Apparatus PhD) through Teflon tubing and then into a stainless-steel capillary (I.D. = 0.047") located 23 cm from a conductive target. High voltage generators (Gamma High Voltage Research) were utilized to charge the PEUU solution at 10 kV and the respective target at -10 kV.

2.3. SMC spraying/electrospraying

Vascular SMCs isolated from rat aorta were expanded on tissue culture polystyrene (TCPS) culture plates under Dulbecco's Modified Eagle Medium (DMEM) supplemented with 10% fetal bovine serum and 1% penicillin-streptomycin [16]. SMCs were sprayed from a sterile air pressurized polypropylene bottle with an attached spray nozzle (Fisher) or electrosprayed from a sterile stainless-steel capillary (I.D. = 0.047") at 10 kV over a distance of 20 cm onto glass slides placed on an aluminum plate charged at -15 kV. To shield cells from processing effects and in an effort to maximize viability, some cell suspensions were supplemented with 3 wt% bovine skin gelatin (Sigma) before spraying or electrospraying. For assessment of cell viability, 50 μ L of sprayed or electrosprayed SMCs in culture medium were added to 50 μ L of 0.4% trypan blue (Gibco). After 5 min incubation, viability was calculated as

$$\% \text{ cell viability} = \frac{\# \text{unstained cells (living)}}{\# \text{total cells (dead+living)}} 100\%.$$

2.4. Microintegration

The first microintegration technique evaluated consisted of simultaneously electrospraying cells and electrospinning PEUU with a side-by-side capillary configuration located 23 cm from the target as depicted in Fig. 1(a). 5×10^6 SMCs/mL in media were fed at 0.25 mL/min with a syringe pump (Harvard Apparatus) through sterile tubing into a sterile capillary charged at 5 kV. PEUU, 5 wt%, was fed at 1.5 mL/hr into a capillary charged at 10 kV. The target was a sterile aluminum plate charged at -10 kV located on an *x-y* stage (Velmex) translating 8 cm along each axis at a speed of 8 cm/s.

In order to fabricate thicker constructs with more uniform cell incorporation, a subsequent microintegration technique was utilized as shown in Fig. 1(b). In this case, SMCs were electrospayed concurrently with PEUU electrospinning using a perpendicular nozzle configuration. A total of 7.5×10^6 SMCs/mL were fed at 0.25 mL/min into a sterile capillary charged at 8 kV and located 5 cm from the target. PEUU, 12 wt%, was fed at 1.5 mL/h into a capillary charged at 10 kV and located 23 cm from the target. The target consisted of a sterile stainless-steel rod (3/4" diameter) charged at 10 kV and rotating at 200 rpm while translating 8 cm along its axis at 8 cm/s. The 5 cm by 5 cm constructs were filleted off the mandrel using a sterile blade by first trimming 1.5 cm off each end before removal. A fabrication time of 45 min was used with both microintegration techniques.

2.5. Cell culture

After fabrication, samples were immediately removed from their respective microintegration targets and placed in a sterile polystyrene dish with a minimal amount of culture medium to cover the sample. Areas of the thin SMC microintegrated sheets fabricated on the flat target that appeared to possess uniform cell integration with electrospun PEUU were punched into 6-mm discs. These discs were cultured statically in poly 2-hydroxyethyl methacrylate (poly HEMA) coated TCPS 96-well plates with 200 μ L of media in each well. As a control, TCPS wells were seeded with SMCs. Media was changed every day.

The thicker constructs fabricated using the mandrel target were characterized initially for uniformity of cellular integration. Samples for subsequent study were first cultured with a minimal amount of media to cover the sample for 4 h to encourage cell adhesion. At this point, cells were considered adherent and an additional 15 mL of media was added to support SMCs for 16 h of static culture. Next, samples were either cultured statically as 6-mm discs in poly HEMA coated TCPS 96-well plates or under transmural perfusion in a custom designed bioreactor. For perfusion culture, samples were cut into 13-mm discs and placed into polypropylene inline filter holders (VWR) between silicone and Teflon o-rings and a support screen. A schematic of the bioreactor as adapted from a previously reported design is shown in Fig. 2 [13]. Each sample was placed in its own flow loop containing a 32-mL media bag (American Fluoroseal Corp), a 2.5-m length of platinum silicone tubing (Cole Parmer, 1/16" I.D.) to serve as a gas exchanger, and two syringes for adding or removing media or bubbles. A multi-channel peristaltic pump (Harvard Apparatus) was utilized to perfuse the loops at 0.5 mL/min. Fifty percent of the media was changed every 2 days.

2.6. Characterization

Quantification of cell viability was achieved using the MTT mitochondrial activity assay ($n = 5$ per sample studied) [17]. Regions exposed to flow from samples removed from the bioreactor were punched into 6-mm discs for MTT. For scanning electron microscopy (SEM) to observe cellular and construct morphologies, samples were rinsed with PBS, fixed with 2.5% glutaraldehyde and 1% osmium tetroxide in PBS and subjected to graded ethanol dehydrations before being critical point dried, sputter-coated and imaged. Samples imaged with fluorescence microscopy were rinsed with PBS, fixed with 2% paraformaldehyde, permeabilized with 0.1% Triton x-100 and stained with rhodamine phalloidin (Molecular Probes) for f-actin and draq-5 (Biostatus Ltd) for nuclei. Imaging was done on a Leica TCS-SL laser scanning confocal microscope. Representative images were taken as individual scans or as a series of stacked images. For sectional histology, samples were fixed in 10% neutral buffered formalin, embedded in paraffin, cross sectioned at 10 μ m and stained with hematoxylin and eosin. Construct tensile mechanical properties immediately after fabrication using the method shown in Fig. 1(b) were measured on an ATS 1101 Universal

Testing Machine (10 mm/min crosshead speed) according to ASTM D638-98 while wetted with media and immediately after removal from a 37 °C incubator.

2.7. Statistics

Results are displayed as the mean \pm standard deviation. One-factor analysis of variance (ANOVA) was utilized to evaluate cell viability, cell growth and mechanical properties using the Neuman-Keuls test for *post hoc* assessments of the differences between samples.

3. Results and discussion

3.1. Polymer characterization

PEUU number average molecular weight was 88 000 and weight average molecular weight was 230 000 as determined by GPC to give a polydispersity of 2.6. DSC values reported a glass transition temperature of -55.0 °C and soft segment melt temperature of 41.0 °C. Cast PEUU film was strong and distensible with a tensile strength of 27 ± 4 MPa and a breaking strain of $820 \pm 70\%$.

3.2. SMC spraying/electrospraying

Electrospinning occurs when a polymer solution is charged to high voltage that generates an electrical force that can extrude out a polymer jet, which then breaks down to sub-micron scale fibers through a complicated bending and whipping process [18]. When solution parameters such as polymer molecular weight, concentration and viscosity are not appropriate to fabricate continuous fibers, electrospinning occurs whereby polymer droplets are deposited on the target [19]. This phenomenon has been investigated for some drug delivery applications [20,21] and some researchers have even electrospayed cells encapsulated within hydrogels and reported no viability loss after exposure to high electrostatic potentials [22].

To evaluate the potential cytotoxic effect of different methods to incorporate cells into electrospun matrices, SMCs were either sprayed from a nozzle under pressure or electrospayed and SMC viability was assessed as a function of each processing variable as shown in Fig. 3. These variables included spraying alone, spraying onto a target charged at -15 kV, spraying onto a target charged at -15 kV with PEUU electrospinning, electrospaying at 10 kV onto a target charged at -15 kV, and electrospaying at 10 kV onto a target charged at -15 kV with PEUU electrospinning. A significant reduction in SMC viability resulted from spraying cells through the nozzle. The physical forces of the pressurized spray in combination with the exposure of cells to processing solvents may have caused this result since viability was lost both from spraying alone and even more so by spraying during electrospun PEUU (e-PEUU) fabrication. Decreased viability from cell aerosol spraying has been reported by others and found to depend largely on nozzle diameter, spray pressure, and solution viscosity [23]. Therefore, cells were also sprayed from media supplemented with gelatin to increase viscosity and help protect the cells from mechanical and chemical stresses. Viability was recovered yet the mechanical integrity of the PEUU matrices was disrupted because of gelation within the fiber network.

In contrast to pressurized spraying, electrospaying cells did not affect cell viability or proliferation. This is consistent with reports by others that cells can survive exposure to high voltage electric fields [22,24]. Even in the presence of PEUU electrospinning, SMC electrospaying viability was not reduced, perhaps because the positively charged electrospinning and electrospaying streams repelled each other and avoided exposing cells to solvent prior to deposition. Also, due to the relatively large electrospinning distance of 23 cm, PEUU fibers were likely free of solvent by the time they were deposited.

Electrospraying from media supplemented with gelatin resulted in reduced construct mechanical properties such that electrospraying from media alone was the preferred cellular incorporation method.

3.3. Microintegration

Initial attempts to microintegrate SMCs into electrospun PEUU consisted of side-by-side electrospraying and electrospinning capillaries and a flat conductive target moving on an x - y stage (Fig. 1(a)). This technique yielded an approximately 100 μm thick construct after 45 min of fabrication. However, the area of electrospraying and electrospinning stream convergence was relatively small such that non-uniformity of cellular integration was an issue. This effect was most likely due to a stream repulsion effect from Coulombic forces [25]. To limit charged stream interactions we modified the apparatus such that the nozzles were located perpendicular to one another and the target was instead a rotating mandrel translating on its axis (Fig. 1(b)). Since the electrospun PEUU and electrosprayed SMC streams were arriving from different directions stream repulsion was minimized and the combination of rotation and translation of the mandrel target induced component mixing even further. This electrospinning nozzle and target configuration may find other applications as a means to fabricate more uniform composite scaffolds by electrospinning multiple materials or introducing drug laden microspheres between fibers. SMC microintegration using this configuration allowed fabrication of approximately 5 cm \times 5 cm construct sheets of thickness ranging from 300 to 500 μm as shown in Fig. 1(c). Scaffold thickness could be controlled by adjusting polymer feedrate or fabrication time. In addition, a more uniform cellular integration was qualitatively visible by observing the overlap of the electrosprayed media and electrospun fibers.

3.4. SMC growth and morphology

SMC growth in thin constructs fabricated as in Fig. 1(a) is summarized in Fig. 4(a). Cell numbers for both sample types increased significantly from 1 day until 1 week in static culture ($p < 0.05$). SMCs on TCPS increased approximately 40% from 1 day until 1 week while those integrated in electrospun PEUU increased by 122% during this period. Fluorescent imaging of SMC microintegrated PEUU indicated that cells remained spherical in shape at 1 h but exhibited the spread morphology after 1 day of static culture (data not shown). SEM micrographs of fixed samples at 1 week exhibited confluent cellular layers present beneath sub-micron diameter PEUU fibers as shown in Fig. 4(b) and (c).

When thicker SMC microintegrated PEUU scaffolds were submitted to this same static culture method, cells did not proliferate within the construct interior. This effect was attributed to poor exchange of nutrients, waste, and oxygen due to diffusional limitations. Also, cells that followed apoptotic or necrotic pathways remaining in the matrix could detrimentally affect the viability of neighboring healthy cells. Thus, a transmural perfusion bioreactor was constructed to allow increased convective and diffusive transport. This bioreactor was adapted from a report by Radisic et al. who engineered contractile cardiac tissue by exposing neonatal cardio-myocytes seeded into collagen sponges to perfusion culture [13]. We hypothesized that this type of culture system would encourage SMC proliferation in our microintegrated constructs and the elastomeric fibers would help retain adherent cells during flow.

Initial SMC densities in thicker constructs fabricated as in Fig. 1(b) and (c) are presented in Fig. 5(a). Cell numbers as measured by MTT immediately after construct fabrication ranged from 8.9×10^4 to 1.6×10^5 cells/well as a function of position. Although no statistically significant difference was found in cell number with position, constructs were trimmed of 1.5 cm from each edge of the mandrel axis prior to further study. Cellular growth over 1

week with static or perfusion culture is summarized in Fig. 5(b). No significant difference in SMC number was found between days 1, 4 or 7 in static culture. However, for samples cultured under transmural perfusion, significantly higher SMC numbers were measured at days 4 and 7 relative to day 1 ($p < 0.05$). These results translate to a 131% and 98% increase in cellular density for perfusion culture versus static culture at days 4 and 7, respectively.

A representative confocal fluorescent image of cellular morphology within the thicker fabricated constructs after 1 day of static culture is shown in Fig. 6(a). SMCs appeared spread and healthy as well as uniformly distributed within the scaffold. In addition, constructs cultured under perfusion exhibited high numbers of spread, healthy appearing cells uniformly located throughout the samples as demonstrated in representative images of Fig. 6(b–d). With perfusion, SMCs were found distributed in greater abundance throughout the fiber matrix as well as deeper beneath the fibers. However, at days 4 and 7 of static culture, as displayed representatively in Fig. 6(e) and (g), the SMCs appeared less abundant as well as exhibited less f-actin staining. Patches of higher cell densities were found at both days 4 and 7 of static culture near the construct surface and not deeper in the fiber network as shown in Fig. 6(f) and (h). The morphology of SMCs at day 7 of static culture did improve slightly in appearance in comparison with day 4.

Hematoxylin and eosin stains of construct cross-sections in Fig. 7 further illustrated the trend of higher cellular density achieved with perfusion culture. One can observe high numbers of layered cells after 1 day of static culture in Fig. 7(a) and (d). Yet, after 4 days of static culture, the cells appear less spread and healthy in Fig. 7(b) and (e). High densities of SMCs microintegrated within the elastomeric fiber network can be observed in Fig. 7(c) and (f) after 4 days of perfusion culture.

As a result of the electrospinning setup that we employed it was possible to induce fiber orientation to influence the cells to organize themselves in an aligned manner. SMCs within the elastomeric fiber matrices qualitatively exhibited an aligned morphology, as seen in Fig. 6(b) for instance. The estimated shear stress to which the SMCs integrated into e-PEUU matrices (at approximately 80% porosity) were exposed in perfusion culture was on the order of 1 dyne/cm² [26]. This shear stress is relatively low and would not be expected to significantly influence cell morphology or decrease viability [27]. We observed SMC orientation to be parallel to the direction of scaffold fiber orientation instead of aligned with the perfusion flow direction.

3.5. Mechanical properties

Tensile mechanical properties of SMC microintegrated PEUU measured immediately after fabrication are summarized in Table 1 and compared with e-PEUU. e-PEUU was found to retain much of the mechanical strength and flexibility of the cast film (reported above). SMC microintegrated PEUU was found to retain a portion of the mechanical strength and distensibility of e-PEUU, with lower tensile strengths and higher breaking strains. This latter result may be due to microintegrated SMCs disrupting the PEUU fiber network and replacing elastic PEUU volume with cellular volume. Yet, the measured properties are still more than sufficient for the SMC microintegrated PEUU to serve as a support structure for soft tissue growth and mechanical training.

As a result of the fabrication process, SMC microintegrated PEUU was found to have tensile properties that differed as a function of the material axis. The axis orientated with the mandrel axis (preferred axis) possessed a significantly higher tensile strength and 100% modulus and a lower breaking strain than the axis orientated with the circumference of the mandrel (cross-preferred axis) ($p < 0.05$). Some degree of fiber alignment in the matrices was induced by a combination of the stage translation speed of 8 cm/s and the mandrel

length to diameter ratio of 8. It was believed that this ratio provided more opportunity for the fibers to deposit parallel to the mandrel axis. Since the mandrel rotation velocity was less (3 cm/s at 200 rpm) than the translation speed, it was not expected to greatly influence fiber alignment. As would be expected, the preferred fiber axis possessed a higher tensile strength and lower breaking strain from a more direct influence on the stretching of the fibrous microstructure of the PEUU. The cross-preferred material axis would be expected to allow more elongation at lower stresses since the mechanical properties would be more influenced by PEUU fiber bending than stretching. By manipulating mandrel rotation and translation rates it should be possible to alter the direction and degree of construct anisotropy. This inherent construct anisotropy and fiber orientation appeared to induce the previously mentioned SMC alignment within the matrices.

4. Conclusions

The relatively rapid creation of a hybrid tissue engineered construct, which is primarily cellular and reinforced with an elastomeric fiber matrix, may offer a meaningful advancement over current tissue engineering approaches. The advantage of high cell densities achieved over short time periods could facilitate the development of functional connections between cells and provide a construct with appropriate cellularity and mechanical properties for soft tissue replacement. The ability to incorporate anisotropy to direct cell morphology is important in both forming functional tissue and mimicking the biomechanics of native aligned tissue structures. This technique might find future application in the engineering of tubular structures, such as a tissue engineered blood vessel, and sheets of elastic tissues for other soft tissue replacement needs.

Acknowledgments

This work was supported by the National Institutes of Health, (#HL069368) and the Commonwealth of Pennsylvania. We acknowledge the staff at the Center for Biologic Imaging at the University of Pittsburgh for their assistance. We also thank Lorenza Draghi, Dr. David Vorp, Dr. Alexandro Nieponce and Dr. Michael Sacks and laboratory for their support and guidance on this project.

References

1. Niklason LE, Gao J, Abbott WM, Hirschi KK, Houser S, Marini R, Langer R. Functional arteries grown in vitro. *Science* 1999;284:489–93. [PubMed: 10205057]
2. L'Heureux N, Paquet S, Labbe R, Germain L, Auger FA. A completely biological tissue-engineered human blood vessel. *FASEB J* 1998;12:47–56. [PubMed: 9438410]
3. Formhals, A. Apparatus for producing artificial filaments from materials such as cellulose acetate. US Patent No 1975504. 1934.
4. Li W, Laurencin CT, Caterson EJ, Tuan RS, Ko FK. Electrospun nanofibrous structure: a novel scaffold for tissue engineering. *J Biomed Mater Res* 2002;60:613–21. [PubMed: 11948520]
5. Shin M, Ishii O, Sueda T, Vacanti JP. Contractile cardiac grafts using a novel nanofibrous mesh. *Biomaterials* 2004;25:3717–23. [PubMed: 15020147]
6. Flemming RG, Murphy CJ, Abrams GA, Goodman SL, Nealey PF. Effects of synthetic micro- and nano-structured surfaces on cell behavior. *Biomaterials* 1999;20:573–8. [PubMed: 10213360]
7. Thapa A, Webster TJ, Haberstroh KM. Nano-structured polymers enhance bladder smooth muscle cell function. *Biomaterials* 2003;24:2915–26. [PubMed: 12742731]
8. Xu CY, Inai R, Kotaki M, Ramakrishna S. Aligned biodegradable nanofibrous structure: a potential scaffold for blood vessel engineering. *Biomaterials* 2004;25:877–86. [PubMed: 14609676]
9. Lee CH, Shin HJ, Cho IH, Kang YM, Kim IA, Park KD, Shin JW. Nanofiber alignment and direction of mechanical strain affect the ECM production of human ACL fibroblast. *Biomaterials* 2005;26:1261–70. [PubMed: 15475056]

10. Guan J, Fujimoto KL, Sacks MS, Wagner WR. Preparation and characterization of highly porous, biodegradable polyurethane scaffolds for soft tissue applications. *Biomaterials* 2005;26:3961–71. [PubMed: 15626443]
11. Li Y, Ma T, Kniss DA, Lasky LC, Yang ST. Effects of filtration seeding on cell density, spatial distribution, and proliferation in nonwoven fibrous matrices. *Biotechnol Prog* 2001;17:935–44. [PubMed: 11587587]
12. Bursac N, Papadaki M, Cohen RJ, Schoen FJ, Eisenberg SR, Carrier R, Vunjak-Novakovic G, Freed LE. Cardiac muscle tissue engineering: toward an *in vitro* model for electrophysiological studies. *Am J Physiol Heart Circ Physiol* 1999;277:H433–44.
13. Radisic M, Yang L, Boublik J, Cohen RJ, Langer R, Freed LE, Vunjak-Novakovic G. Medium perfusion enables engineering of compact and contractile cardiac tissue. *Am J Physiol Heart Circ Physiol* 2004;286:H507–16. [PubMed: 14551059]
14. Guan J, Sacks MM, Beckman EJ, Wagner WR. Synthesis, characterization, and cytocompatibility of elastomeric, biodegradable poly(ester-urethane)ureas based on poly(caprolactone) and putrescine. *J Biomed Mater Res* 2002;61:493–503. [PubMed: 12115475]
15. Stankus JJ, Guan J, Wagner WR. Fabrication of biodegradable elastomeric scaffolds with sub-micron morphologies. *J Biomed Mater Res* 2004;70:603–14.
16. Ray JL, Leach R, Herbert JM, Benson M. Isolation of vascular smooth muscle cells from a single murine aorta. *Methods Cell Sci* 2002;23:185–8. [PubMed: 12486328]
17. Ohno M, Abe T. Rapid colorimetric assay for the quantification of leukemia inhibitory factor (LIF) and interleukin-6 (IL-6). *J Immunol Meth* 1991;145:199–203.
18. Shin YM, Hohman MM, Brenner MP, Rutledge GC. Electrospinning: a whipping fluid jet generates submicron polymer fibers. *App Phy Let* 2001;78:1149–51.
19. Grace JM, Marijnissen JCM. A review of liquid atomization by electrical means. *J Aerosol Sci* 1994;25:1005–19.
20. Reyderman L, Stavchansky S. Electrostatic spraying and its use in drug deliver—cholesterol microspheres. *Int J Pharm* 1995;124:75–85.
21. Ijsebaert JC, Geerse KB, Marijnissen JCM, Lammers JJ, Zanen P. Electro-hydrodynamic atomization of drug solutions for inhalation purposes. *J Appl Physiol* 2001;91:2735–41. [PubMed: 11717241]
22. Nedovic VA, Obradovic B, Poncelet D, Goosen MFA, Leskosek-Cukalovic O, Bugarski B. Cell immobilization by electrostatic droplet generation. *Landbauforsch Volk* 2002;241:11–7.
23. Veazey WS, Anusavice KJ, Moore K. Mammalian cell delivery via aerosol deposition. *J Biomed Mater Res* 2005;72B:334–8.
24. Temple, MD.; Bashari, E.; Lu, J.; Zong, WX.; Thompson, CB.; Pinto, NJ.; Manohar, SK.; King, RCY.; MacDiarmid, AG. Electrostatic transportation of living cells through air. Abstracts of Papers, 223rd ACS National Meeting; Orlando, FL. April 7–11 2002;
25. Theron SA, Yarin AL, Zussman E, Kroll E. Multiple jets in electrospinning: experiment and modeling. *Polymer* 2005;46:2889–99.
26. Carrier RL, Rupnick M, Langer R, Schoen FJ, Freed LE, Vunjak-Novakovic G. Perfusion improves tissue architecture of engineered cardiac muscle. *Tiss Eng* 2002;8:175–88.
27. Stathopoulos NA, Lellums JD. Shear stress effects on human embryonic kidney cells *in vitro*. *Biotechnol Bioeng* 1985;27:1021–6. [PubMed: 18553772]

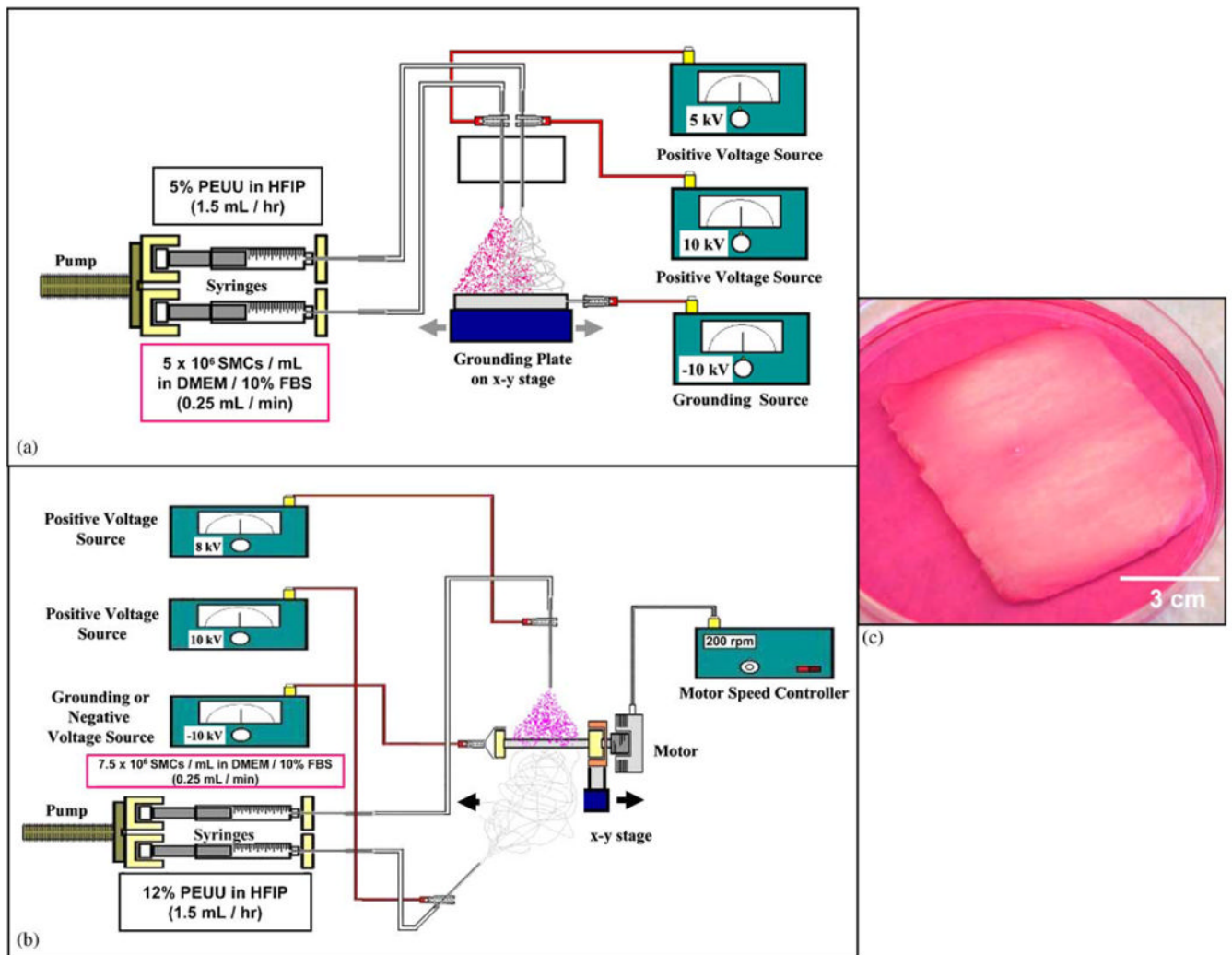


Fig. 1. Approaches to cellular microintegration. (a) Microintegration using a side-by-side capillary configuration for electrospinning polymer and electrospraying cells onto a flat target moving on an x - y stage. (b) Microintegration using a perpendicular capillary configuration for electrospinning polymer and electrospraying cells onto a rotating mandrel moving on a linear stage to result in the construct shown in (c).

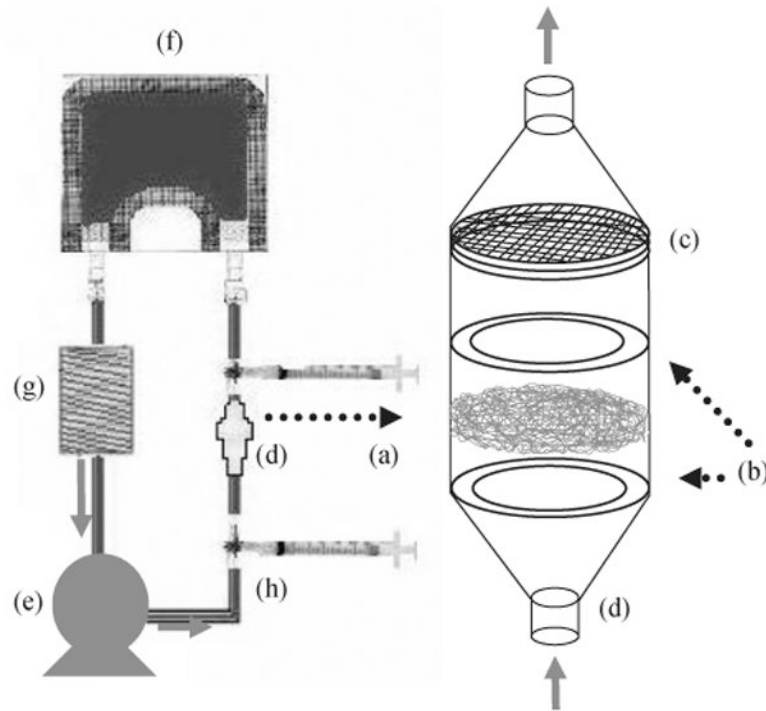


Fig. 2. Schematic of the perfusion bioreactor employed with microintegrated constructs. 13 mm diameter construct discs (a) were placed between O-rings (b) and a support screen (c) of in-line filter holders (d) followed by perfusion at 0.5 mL/min with a multi-channel peristaltic pump (e). Each construct was placed in its own loop consisting of a 32 mL media bag (f), silicone tubing gas exchanger (g) and syringes for media exchange (h).

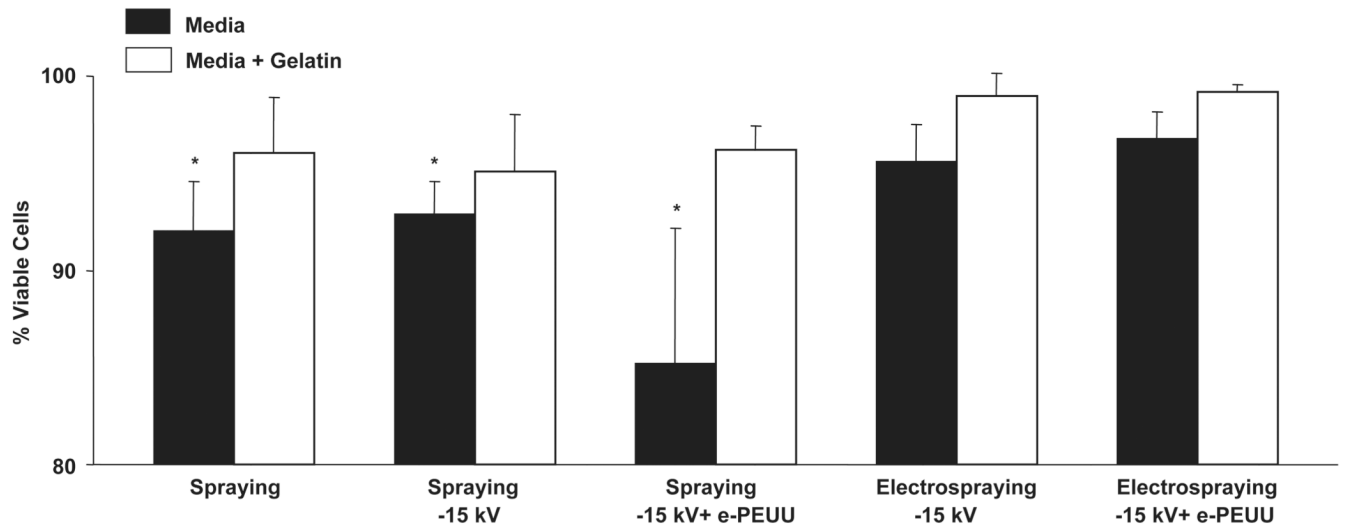


Fig. 3.

Trypan blue staining results for SMC viability after various processing treatments (Spraying = SMCs sprayed from spray nozzle, Spraying -15 kV = SMCs sprayed from spray nozzle onto -15 kV charged target, Spraying -15 kV + e-PEUU = SMCs sprayed from spray nozzle onto -15 kV charged target during PEUU electrospinning, Electrospraying -15 kV = SMCs electrospayed at 10 kV onto -15 kV charged target, Electrospraying -15 kV + e-PEUU = SMCs electrospayed at 10 kV onto -15 kV charged target during PEUU electrospinning).

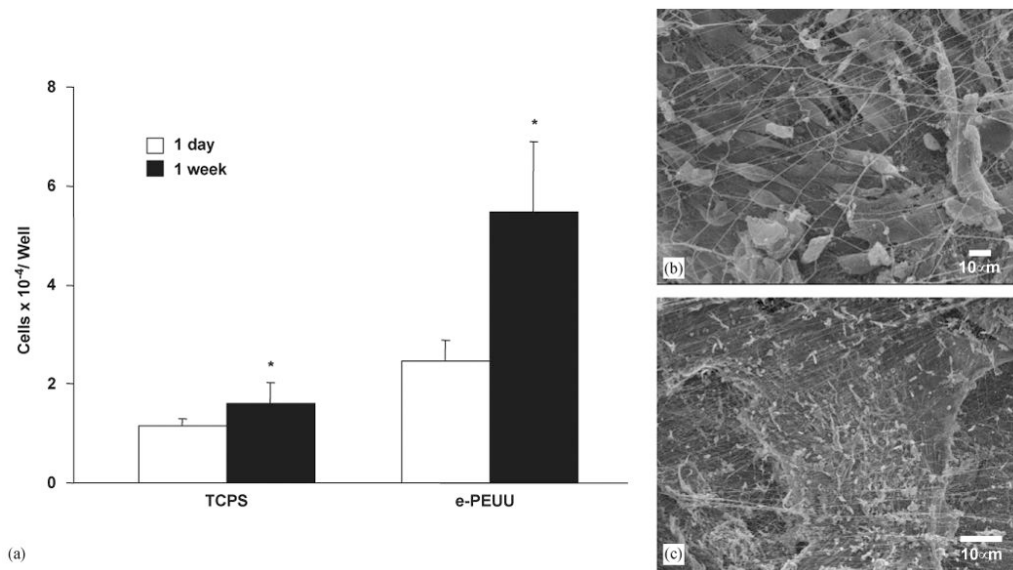


Fig. 4. (a) Cell growth in thin SMC microintegrated e-PEUU construct fabricated on a flat target versus TCPS over 1 week in static culture (* $p < 0.05$ increase from 1 day to 1 week). (b) and (c) Representative electron micrographs of SMC microintegrated samples from (a) at 1 week in culture. ((b) scale bar = 10 μm , (c) scale bar = 100 μm).

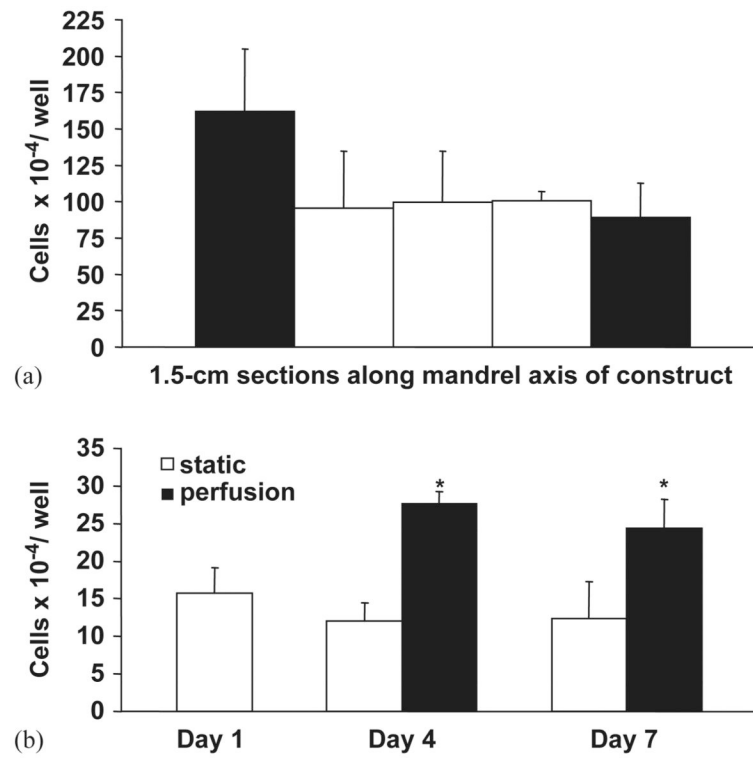


Fig. 5. (a) Initial cellular uniformity in SMC microintegrated e-PEUU fabricated on a mandrel target. (b) Cell growth in thick SMC microintegrated e-PEUU constructs with static versus perfusion culture. Perfusion was initiated after 1 day in static culture. (* $p < 0.05$ increase with perfusion versus static culture).

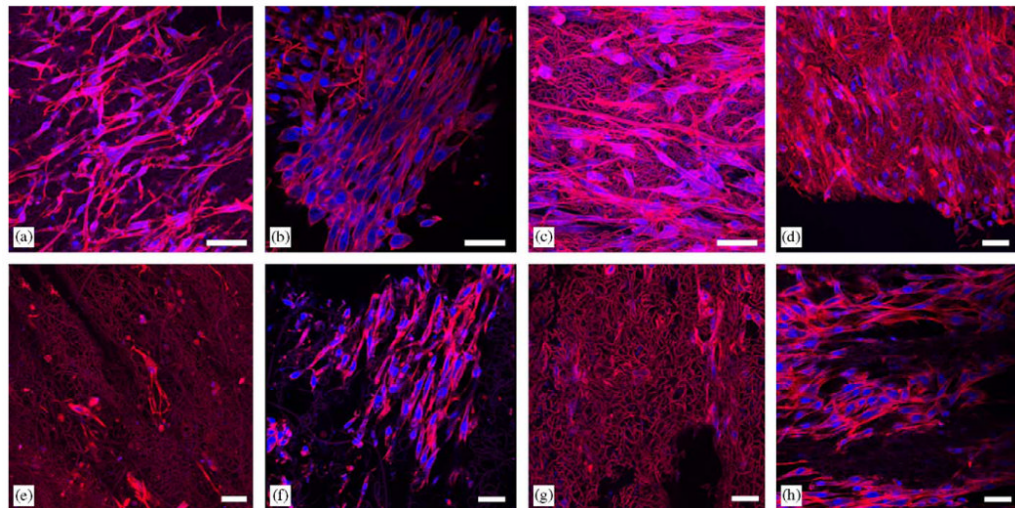


Fig. 6. Fluorescent micrographs of SMC microintegrated e-PEUU constructs after one day of static culture (a), day 4 of perfusion culture (b), day 4 of perfusion culture (c), day 7 of perfusion culture (d), day 4 of static culture (e), high cell number surface image of day 4 of static culture (f), day 7 of static culture (g), and high cell number surface image of day 7 of static culture (h). (scale bar = 40 μ m, red = f-actin and e-PEUU, blue = nuclei).

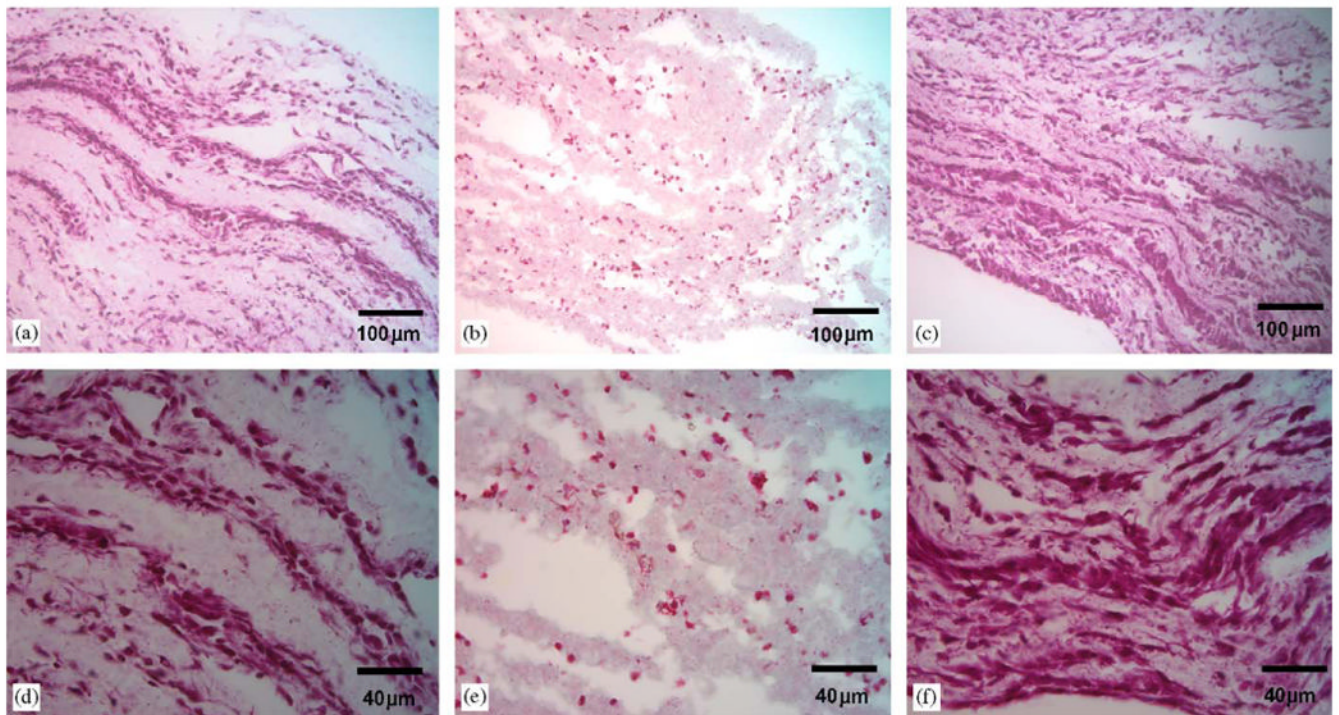


Fig. 7. Hematoxylin and eosin stained sections of SMC microintegrated e-PEUU constructs after one day of static culture (a, c), day 4 of static culture (b, e), and day 4 of perfusion culture (c, f). ((a–c) scale bar = 100 μm , (d–f) scale bar = 40 μm).

Table 1

Tensile Properties of SMC microintegrated PEUU

Sample	Initial modulus (MPa)	100% modulus (MPa)	Tensile strength (MPa)	Breaking strain (%)
e-PEUU (random)	2.5 ± 1.2	2.8 ± 1.1	8.5 ± 1.8	280 ± 40
μSMC-e-PEUU (preferred)	1.7 ± 0.2	1.4 ± 0.2	6.5 ± 1.6	850 ± 200
μSMC-e-PEUU (cross-preferred)	—	0.3 ± 0.1	2.0 ± 0.5	1700 ± 100

e = electrospun scaffold; μSMC = SMC microintegrated.